Available online at www.sciencedirect.com
SCIENCE DIRECT®
Journal of Sound and Vibration 286 (2005) 145–165
JOURNAL OF SOUND AND VIBRATION
www.elsevier.com/locate/jsvi

Equivalent electric circuits of thin plates with two-dimensional piezoelectric actuators

Guo-Qing Li*, Chen Chuan-Yao, Hu Yuan-Tai

School of Civil Engineering and Mechanics, Huazhong University of Science and Technology, Wuhan 430074, Hubei, PR China

Received 16 January 2004; received in revised form 31 August 2004; accepted 1 October 2004
Available online 19 December 2004

Abstract

Electrical equivalent circuits with impedance elements modeling the electromechanical behavior of a thin plate with piezoelectric actuators are presented. The dynamic characteristics of a two-dimensional piezoelectric force actuator are represented by a 5×5 impedance matrix, which is equivalent to a five-port electric network. When the dual piezoelectric actuators are assumed to produce average bending moments for a unit length along the edge at the interfacial surfaces, a 5×5 impedance matrix for these actuators is obtained. While the dual actuators are assumed to produce average bending moments for a unit area at the interfacial surfaces between the plate and the actuators, a 3×5 impedance matrix is presented. According to the theory of thin plates, the impedance of a rectangle thin plate with four simply supported edges is related with vibration amplitude of the plate. The continuity conditions between the actuators and the plates are established by using two approximate hypotheses we proposed. The system impedances are finally obtained by solving the impedance equations of the piezoelectric actuators and the plate. Four numerical examples are analyzed to illustrate the application of this modeling method, and the results agree well with the results obtained by other methods. Equivalent electric circuits of thin plates with piezoelectric actuators are capable of dynamically analyzing of such complex electromechanical system with 2D piezoelectric actuators.

*Corresponding author. Tel.: +86 27 87541715; fax: +86 27 87543501.
E-mail address: lig57@mail.hust.edu.cn (G.-Q. Li).

0022-460X/$ - see front matter © 2004 Elsevier Ltd. All rights reserved.
doi:10.1016/j.jsv.2004.10.001

1. Introduction

The smart structures integrated with piezoelectric sensors and/or actuators are widely investigated in recent years. The theories and methodologies for such structures are on the basic knowledge in this field, which is the fundamental in designing and manufacturing smart structures with piezoelectric materials. Models for studying the interaction of piezoelectric actuators to structures have been intensively studied since 1980s. Crawley and De Luis [1] proposed a static model to analyze the smart beams surface-mounted with piezoelectric actuators, which are assumed to produce pure bending activation, and they analyzed the thin plate driven by induced-strain actuators in a quasi-static way, in which the inertial or mass of the actuators are not included in their model. Park et al. [2] extended this type of models into the case of piezoelectric actuators that produce beading and torsion. Further more, Lim and He [3] obtained the exact solution of a compositionally graded piezoelectric layer under uniform stretch, bending and twisting recently. Liang et al. [4,5] first proposed impedance models for smart beams and plates, where the elastic structures and piezoelectric actuators are represented by one or two two-dimensional (2D) impedance elements in their models. The dynamic equilibriums at the connection between the elastic and piezoelectric elements are formulated. They proposed a dynamic actuator/structure interaction chart (DASIC) in analyzing 1D smart beam with a PZT stack [4]. These impedance models are also used to determine the power flow and consumption [6], to optimize the locations of the actuators [7] and to calculate the thermal effect in smart structures [5]. Dimitriadis [8], Zhou [9] and their co-workers studied the vibration of beam, thin plates and cylindrical vessel driven by piezoelectric actuators both theoretically and experimentally using impedance models. Although the concepts of static and dynamic equilibrium are clearly clarified in impedance models, the corresponding relationships of the electromechanical continuity conditions to the actual connections between 2D actuators and structures are inexplicably modeled in their models.

The equivalent electric circuits of mechanical systems such as acoustic system has been proved to be successful in the history [10,11], and it tends to be a good methodology for modeling electromechanical system including smart structures with piezoelectric actuators. This methodology is based on the accordance of governing differential equations between the actual electromechanical system and electric system [10]. Recently, Aoyagi and Tanaka [12] have obtained an equivalent electric model for a smart beam with dual piezoelectric actuators, which produce pure bending to the host structure. They used a group of impedance equations to present the beam vibration of multiple degrees of freedom (mdof). They also analyzed a piezoelectric acceleration sensor using equivalent electric circuits and vibration modal superposition method in their research [13]. Li Guo-Qing et al. [14,15] proposed some simple equivalent electric circuits for analyzing smart beams and plates supported by piezoelectric stacks. Cho and his co-workers [16] proposed a five-port equivalent electric circuit when they investigated the piezoelectric bimorphs, and the 3D solution of such smart structures has been obtained by Lim et al. [17]. The five-port electric network proposed by Cho et al. can be used to analyze piezoelectric bimorphs with arbitrary boundary conditions, including clamped, simply supported and free boundary conditions.

Most of the equivalent electric models established before are of smart beams or plates only with 1D actuators, which can be equivalently modeled as electric networks with a few ports. But 2D

piezoelectric actuators actually produce distributed activations in plates, which has been revealed by both FEM analysis and experiments, and the early works by Tzou et al. [18] and Ha et al. [19] using FEM and the experimental works by Zhou et al. are some of the instances. Then, the dynamic characteristics of two-dimensional piezoelectric actuators will be exclusively studied in the following section of this paper. As one two-dimensional piezoelectric actuator work as a force actuator, the equivalent electromechanical efforts and flows will be well defined. An impedance matrix of this actuator and the equivalent multi-port electric network are presented. As a pair of 2D piezoelectric actuator is used as actuators to produce pure bending, the equivalent mechanical efforts can be defined as the average bending moments for a unit edge length or for a unit contact area of the actuators. The impedances of these actuators are obtained and their corresponding equivalent electric networks are presented as well. As far as the host elastic structures are concerned, it will be not difficult to analyze the impedance of a rectangle plate with various edge boundary conditions using the vibration theory of thin plates.

Another difficulty of establishing the equivalent electric models is to deal with the complicated boundary conditions involved with plates or shells with 2D actuators. To deal with the continuity conditions at the interfacial surfaces between the actuators and the plates, two approximate hypotheses are proposed in this paper. One hypothesis is to average the actual distributed bending actuation and the other is to relate the edge velocities of 2D rectangle actuators with the deflection velocity of thin plate. Once the equivalent electric systems of 2D piezoelectric actuators and thin plate are obtained, dynamic characteristics of the equivalent electric system considered are analyzed in detail. At the end of this paper, several examples are presented to illustrate the applications of the proposed methods using equivalent electric networks.

2. Equivalent electric circuits of 2D piezoelectric actuators

2.1. Impedance equation of a 2D force actuator

Let us consider a generic model of a 2D piezoelectric element integrated with a structure as shown in Fig. 1a. It is assumed that when an AC voltage is applied across a piezoelectric element along the polarization direction, an in-plane expansion (or contraction) is induced in both $1(x_p)$ and $2(y_p)$ axes of the patch. The dynamic response of the element should be solved from its constitutive equations and the geometric boundary conditions, so that the displacement response of the piezoelectric actuator may be described by [4]

$$u_p = [A\ \sin(k_{p11}x_p) + B\ \cos(k_{p11}x_p)]\mathrm{e}^{\mathrm{j}\omega t},$$
$$v_p = [C\ \sin(k_{p22}y_p) + D\ \cos(k_{p22}y_p)]\mathrm{e}^{\mathrm{j}\omega t}, \tag{1}$$

where ω is the working frequency and $\mathrm{j} = \sqrt{-1}$. The subscript p refers to the parameters of the piezoelectric element, which will be always implicit in this paper. In the above equation the wavenumbers k_{p11} and k_{p22} are identical for isotropic piezoelectric materials [4]:

$$k_p^2 = k_{p11}^2 = k_{p22}^2 = \omega^2 \frac{\rho_p}{Y_p^E}, \tag{2}$$

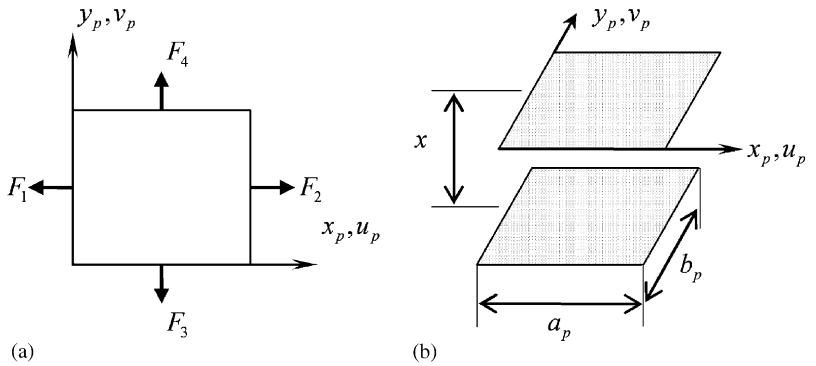

Fig. 1. 2D piezoelectric actuators: (a) one piezoelectric 2D force actuator; (b) dual piezoelectric 2D bending actuators.

in which ρ_p and Y_p^E denote the mass density and Young's modules of the actuator, respectively. The constants A, B, C and D are determined by boundary conditions of the piezoelectric actuator. Then, the strains of the piezoelectric actuators should be

$$\varepsilon_{px} = [A\cos(k_{p11}x_p) - B\sin(k_{p11}x_p)]k_{p11}e^{j\omega t},$$
$$\varepsilon_{py} = [C\cos(k_{p22}y_p) - D\sin(k_{p22}y_p)]k_{p22}e^{j\omega t}. \tag{3}$$

According to the analogy theory between the electric systems and the mechanical systems, the mechanical velocities are analogy to electric flows (so that it can be called as mechanical flows) while the mechanical forces are analogy to electric efforts (mechanical efforts). Therefore, the mechanical flows of the piezoelectric actuator can be defined by the edge velocities of the 2D piezoelectric actuator,

$$U_1 = \left.\frac{\partial u_p}{\partial t}\right|_{x_p=0}, \quad U_2 = \left.\frac{\partial u_p}{\partial t}\right|_{x_p=a_p}, \quad U_3 = \left.\frac{\partial v_p}{\partial t}\right|_{y_p=0}, \quad U_4 = \left.\frac{\partial v_p}{\partial t}\right|_{y_p=b_p}. \tag{4}$$

Substituting Eq. (1) into Eq. (4), the constants A, B, C and D are expressed in terms of the mechanical flows,

$$A = \frac{U_2}{j\omega e^{j\omega t}\sin(k_{p11}a_p)} - \frac{U_1\cos(k_{p11}a_p)}{j\omega e^{j\omega t}\sin(k_{p11}a_p)},$$
$$B = \frac{U_1}{j\omega e^{j\omega t}},$$
$$C = \frac{U_4}{j\omega e^{j\omega t}\sin(k_{p22}b_p)} - \frac{U_3\cos(k_{p22}b_p)}{j\omega e^{j\omega t}\sin(k_{p22}b_p)},$$
$$D = \frac{U_3}{j\omega e^{j\omega t}}. \tag{5}$$

It is assumed that $V = \bar{V}e^{j\omega t}$ is the electric field applied across the thickness of the actuator. The over bar over the symbol refers to the spatial component of the variable, which will also be always

implicit in this paper. Thus, the electric field in the thickness direction is given by

$$E = \bar{V} e^{j\omega t}/t_p, \tag{6}$$

where t_p is the thickness of the actuator.

Next the constitutive equations of the piezoelectric actuator is used to determinate the mechanics efforts by electric and displacement fields. The stresses σ_{px}, σ_{py} and electric displacement D_z are

$$\begin{aligned}
\sigma_{px} &= \frac{Y_p^E}{1-v_p^2}[(\varepsilon_{px} - d_{31}E) + v_p(\varepsilon_{py} - d_{32}E)],\\
\sigma_{py} &= \frac{Y_p^E}{1-v_p^2}[(\varepsilon_{py} - d_{32}E) + v_p(\varepsilon_{px} - d_{31}E)],\\
D_z &= \mu_{33}E + d_{31}\sigma_{px} + d_{32}\sigma_{py},
\end{aligned} \tag{7}$$

where d_{31} and d_{32} are the piezoelectric constants, v_p denotes Poisson's ratio of the actuator, and μ_{33} is the dielectric permittivity constant.

The electric current passing through the piezoelectric actuator is thus given by

$$I = \int_0^{b_p}\int_0^{a_p} \dot{D}_z \, dx_p \, dy_p, \tag{8}$$

where a_p and b_p are length and width of the piezoelectric actuator, respectively. Next, we define the mechanical efforts as

$$\begin{aligned}
F_1 &= -\frac{t_p}{b_p}\int_0^{b_p} \sigma_{px}\, dy_p\Big|_{x_p=0}, \quad F_2 = \frac{t_p}{b_p}\int_0^{b_p} \sigma_{px}\, dy_p\Big|_{x_p=a_p},\\
F_3 &= -\frac{t_p}{b_p}\int_0^{b_p} \sigma_{py}\, dx_p\Big|_{y_p=0}, \quad F_4 = \frac{t_p}{b_p}\int_0^{b_p} \sigma_{py}\, dx_p\Big|_{y_p=b_p}.
\end{aligned} \tag{9}$$

The sign convention of the variables in the above equations are shown in Fig. 1a. Substituting the third equation of Eq. (7) together with Eqs. (6), (5) and (3) into Eq. (8) yields the relation between electric current and mechanical flows, which are Eq. (A.1) shown in the appendix.

To sum up the above formulations, the electromechanical flows of 2D piezoelectric actuator are

$$\mathbf{U}_A = \{U_1, U_2, U_3, U_4, I\}^{\mathrm{T}}, \tag{10}$$

while the electromechanical efforts are defined by

$$\mathbf{F}_A = \{F_1, F_2, F_3, F_4, V\}^{\mathrm{T}}. \tag{11}$$

After a long but not very complex calculations using the above 11 equations, the actuator impedance relationship between electromechanical efforts and electromechanical flows is obtained, that is

$$\mathbf{F}_A = \mathbf{Z}_A \mathbf{U}_A, \tag{12}$$

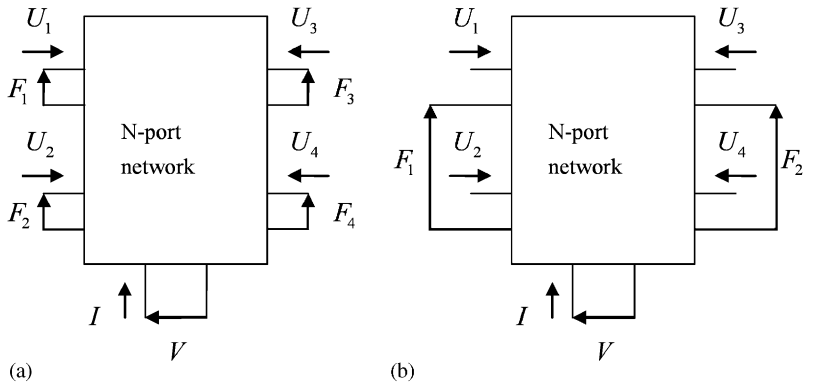

Fig. 2. Equivalent electric networks for 2D piezoelectric actuators: (a) five-port equivalent electric network for 2D force actuator; (b) five-port equivalent electric network for 2D bending actuators.

where $\mathbf{Z}_A$ is an 5×5 impedance matrix, whose elements are listed in the appendix. It should be noted that the above equation governs the dynamic behavior of a piezoelectric actuator shown in Fig. 1a, therefore, Eq. (11) can be called 'impedance equation of a 2D dimensional force actuator'. The electric equivalent network for Eq. (11) is a five-port network shown in Fig. 2a. It should be mentioned that Brissaud [20] has given a 7×7 impedance matrix using a similar formulism to the above when he studied 3D modeling for a rectangle piezoelectric plate.

2.2. Impedance equation of dual bending actuators

In many cases of smart structures integrated with the piezoelectric actuators, a pair of piezoelectric actuators is used to produce pure bending activation as shown in Fig. 1b. It is assumed that the two patches of piezoelectric actuators are completely symmetry, and the voltages applied on the top and the bottom surface of the piezoelectric electrodes are counter-wise to each other. In the following, we will investigate the dynamic behavior of such dual piezoelectric actuators and give their corresponding equivalent electric models.

At first, by examining Eq. (3) and the first two equations of Eq. (7), the stress distributions in the actuators should be a distribution function along $1(x_p)$ and $2(y_p)$ axes directions. The dual actuators actually apply distributed bending moments to the plate, which can be described as

$$m_x(x_p, y_p) = t_p(t_p + t_s)\sigma_{px}, \quad m_y(x_p, y_p) = t_p(t_p + t_s)\sigma_{px}, \tag{13}$$

where t_s denotes the thickness of the structural plate. In order to simplify the model and formula, we seek the expressions of the average bending actuation to replacing the actuation given by Eq. (13) in the following.

We adopt the assumption that the distributed moments of bending along one edge line of the actuator can be regarded as a constant, which is proposed by Crawley and Lazarus [21]. Thus, the average bending moments for a unit length along the axes directions at the edges of the plate

are introduced:

$$M_{x0} = -\frac{t_p(t_s+t_p)}{b_p}\int_0^{b_p}\sigma_{px}\,\mathrm{d}y_p\bigg|_{x_p=0}, \quad M_{xa} = \frac{t_p(t_s+t_p)}{b_p}\int_0^{b_p}\sigma_{px}\,\mathrm{d}y_p\bigg|_{x_p=a_p},$$
$$M_{y0} = -\frac{t_p(t_s+t_p)}{a_p}\int_0^{a_p}\sigma_{py}\,\mathrm{d}x_p\bigg|_{y_p=0}, \quad M_{yb} = \frac{t_p(t_s+t_p)}{a_p}\int_0^{a_p}\sigma_{py}\,\mathrm{d}x_p\bigg|_{y_p=b_p}. \tag{14}$$

Then, the average bending moments given by Eq. (14) combined with electric voltage can be defined as equivalent electromechanical efforts in this case, which are

$$\mathbf{F}_B = \{M_{x0}, M_{xa}, M_{y0}, M_{yb}, V\}^{\mathrm{T}}. \tag{15}$$

While the definition of electromechanical flows in Eq. (10) keeps unchanged and the definitions of mechanical efforts are given by Eq. (15), the impedance matrix for the dual actuators will become

$$\mathbf{F}_B = \mathbf{Z}_B\mathbf{U}_A, \tag{16}$$

where $\mathbf{Z}_B$ is an impedance matrix, which are related with $\mathbf{Z}_A$ by the following equations:

$$Z_{Bij} = (t_p + t_s)Z_{Aij} \quad (i = 1, 4,\ \ j = 1, 5),$$
$$Z_{B5j} = Z_{A5j} \quad (j = 1, 5). \tag{17}$$

Since Eq. (17) represents the dynamic behavior of dual piezoelectric actuators producing average bending moments on a unit length along the axes directions to the 2D structures, Eq. (16) can be called 'impedance equation of dual bending line actuators'. In this case, the electric equivalent network for Eq. (17) is also a five-port network shown in Fig. 2a but the impedance of the network $\mathbf{Z}_A$ should be replaced by $\mathbf{Z}_B$. In the global coordinate system, the load function of the dual actuators can be written as

$$M_x = [M_{x0}\delta(x - x_0) - M_{xa}\delta(x - x_a)][H(y - y_0) - H(y - y_b)],$$
$$M_y = [M_{y0}\delta(y - y_0) - M_{yb}\delta(y - y_b)][H(x - x_0) - H(x - x_a)]. \tag{18}$$

where x and y are axes of the global coordinates system originated in the host structure, and $H(\bullet)$ is a unit step function and $\delta(\bullet)$ is a delta function. These bending activations are illustrated in Fig. 3a.

Another more simple model for dual 2D piezoelectric actuators can be used, in which the dual piezoelectric actuators are assumed to produce the average area bending moments to the host structures. Therefore, the bending moments for a unit area of the interfacial surface between the actuators and the plate can also be defined as mechanical efforts, which are

$$M_{px} = \frac{t_p(t_s+t_p)}{a_p b_p}\int_0^{b_p}\int_0^{a_p}\sigma_{px}\,\mathrm{d}x_p\,\mathrm{d}y_p,$$
$$M_{py} = \frac{t_p(t_s+t_p)}{a_p b_p}\int_0^{b_p}\int_0^{a_p}\sigma_{py}\,\mathrm{d}x_p\,\mathrm{d}y_p. \tag{19}$$

The equivalent electromechanical efforts vector in this case is

$$\mathbf{F}_C = \{M_{px}, M_{py}, V\}^{\mathrm{T}}. \tag{20}$$

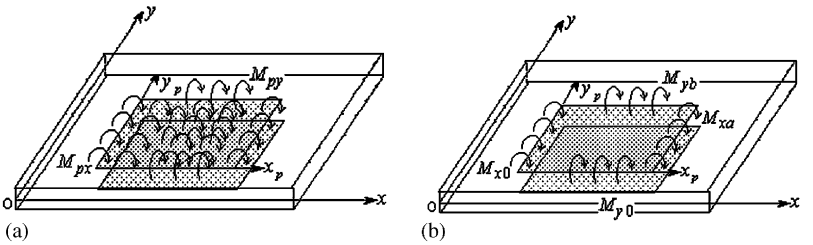

Fig. 3. Models for the bending activation of dual 2D piezoelectric actuators: (a) dual piezoelectric 2D actuators producing line bending moments; (b) dual piezoelectric 2D actuators producing area bending moments.

Following the same procedure to obtain Eq. (16), the following expression between the average bending moment activation and mechanical flows are also obtained.

$$\mathbf{F}_C = \mathbf{Z}_C \mathbf{U}_A, \tag{21}$$

where the elements of 3×5 impedance matrix $\mathbf{Z}_C$ are also listed in the appendix. Eq. (21) represents the dynamic behavior of dual piezoelectric actuators producing average bending activation for a unit area of the plate, so Eq. (21) can be called 'impedance equation of dual bending area actuators'. In this case, these actuations are illustrated in Fig. 3b. The equivalent electric network for Eq. (21) should be a five-port network with two short close circuit as shown in Fig. 2b and the activation function should be

$$\begin{aligned} M_x &= M_{px}[H(x-x_0) - H(x-x_a)][H(y-y_0) - H(y-y_b)], \\ M_y &= M_{py}[H(x-x_0) - H(x-x_a)][H(y-y_0) - H(y-y_b)]. \end{aligned} \tag{22}$$

3. Equivalent electric circuits of thin plate with piezoelectric actuators

Consider the vibration problems of a rectangle thin plate driven by a pair of rectangle piezoelectric actuators as shown in Fig. 4. The theory of thin plates is adopted, and the equation of motion for rectangle plate can be expressed as follows:

$$\begin{aligned} &D_s \nabla^2 \nabla^2 w + \rho_s t_s \frac{\partial^2 w}{\partial t^2} + \bar{c}_s \frac{\partial w}{\partial t} = f(x,y,t), \\ &D_s = \frac{Y_s t_s^3}{12(1-v_s^2)}, \\ &\nabla^2 = \frac{\partial^2}{\partial x^2} + \frac{\partial^2}{\partial y^2}, \end{aligned} \tag{23}$$

where ρ_s is the mass density of the plate and t_s the thickness, Y_s and v_s denote Young's modules and Poisson's ratio of the structural plate, respectively. The subscript s refers to the parameters of the structural thin plate, which will be always implicit. As driving by voltage $V = \bar{V} e^{j\omega t}$ on a pair of actuators on the top and bottom surfaces of the plate, the system response is also harmonic and

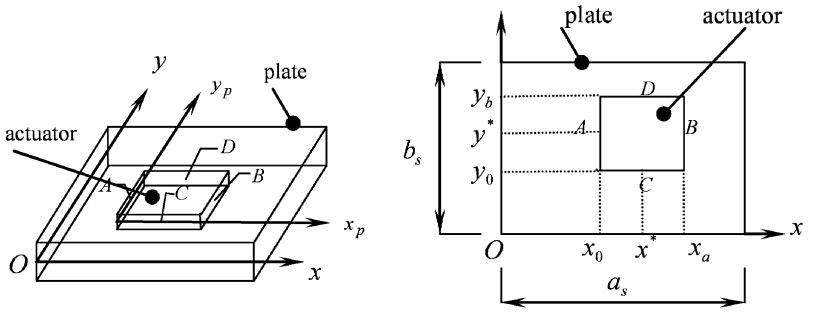

Fig. 4. Geometry configuration of a simply supported thin plate actuated by a pair of 2D actuators.

is written as follows:

$$w(x,y,t)=\sum_{m=1}^{\infty}\sum_{n=1}^{\infty}\bar{W}_{mn}\phi_{mn}(x,y)\mathrm{e}^{\mathrm{j}\omega t}. \tag{24}$$

The vibration mode function of the thin plate with four simply supported edges is

$$\begin{aligned}&\phi_{mn}(x,y)=\sin\ \alpha_m x\ \sin\alpha_n y,\\ &\alpha_m=\frac{m\pi}{a_s},\quad \alpha_n=\frac{n\pi}{b_s},\end{aligned} \tag{25}$$

where a_s and b_s are the length and the width of the plate. Inserting Eq. (25) into Eq. (24) leads to

$$\sum_{m=1}^{\infty}\sum_{n=1}^{\infty}\{D_s(\alpha_m^2+\alpha_n^2)^2-\omega^2\rho_s t_s+\mathrm{j}\omega\bar{c}_s\}\bar{W}_{mn}\phi(x,y)=\bar{f}(x,y). \tag{26}$$

Provided that damping coefficient $\bar{c}_s$ is set to zero, Eq. (26) can be rewritten as

$$\sum_{m=1}^{\infty}\sum_{n=1}^{\infty}(\omega_{mn}^2-\omega^2)\bar{W}_{mn}\phi(x,y)=\frac{1}{\rho_s t_s}\bar{f}(x,y), \tag{27}$$

where the resonant frequencies ω_{mn} are given by

$$\omega_{mn}=\pi^2\left(\frac{m^2}{a_s^2}+\frac{n^2}{b_s^2}\right)\sqrt{\frac{D_s}{\bar{m}}}, \tag{28}$$

in which $\bar{m}$ is mass of the plate per area. Recalling the actuation function of piezoelectric actuators given by Eq. (18), the spatial component of the bending moments are

$$\begin{aligned}\bar{M}_x&=[\bar{M}_{x0}\delta(x-x_0)-\bar{M}_{xa}\delta(x-x_a)][H(y-y_0)-H(y-y_b)],\\ \bar{M}_y&=[\bar{M}_{y0}\delta(y-y_0)-\bar{M}_{yb}\delta(y-y_b)][H(x-x_0)-H(x-x_a)].\end{aligned} \tag{29}$$

The load function of the bending moments is

$$\bar{f}(x,y)=\frac{\partial^2\bar{M}_x}{\partial x^2}+\frac{\partial^2\bar{M}_y}{\partial y^2}. \tag{30}$$

Substituting Eq. (29) into Eq. (30) and then inserting to Eq. (27), the vibration amplitude of the plate is obtained, which is

$$\bar{W}_{mn} = \frac{4}{a_s b_s t_s \rho_s (\omega_{mn}^2 - \omega^2)\alpha_m \alpha_n} \times \{\alpha_m^3 (\bar{M}_{xa} \sin \alpha_m x_a - \bar{M}_{x0} \sin \alpha_m x_0)(\cos \alpha_n y_b - \cos \alpha_n y_0)) + \alpha_n^3 (\bar{M}_{yb} \sin \alpha_n y_b - \bar{M}_{y0} \sin \alpha_n y_0)(\cos \alpha_m x_a - \cos \alpha_m x_0)\}. \quad (31)$$

In the case of vibration of the plate driven by the area actuation given by Eq. (22), the spatial components of bending moments are expressed as follows:

$$\bar{M}_x = \bar{M}_{px}[H(x - x_{p0}) - H(x - x_{pa})][H(y - y_{p0}) - H(y - y_{pb})],$$
$$\bar{M}_y = \bar{M}_{py}[H(x - x_{p0}) - H(x - x_{pa})][H(y - y_{p0}) - H(y - y_{pb})]. \quad (32)$$

Similarly, the vibration amplitude of the plate produced by piezoelectric area actuators are solved from Eq. (32) by using Eq. (32), which is

$$\bar{W}_{mn} = \frac{4(M_{px}\alpha_m^2 + M_{py}\alpha_n^2)}{a_s b_s t_s \rho_s (\omega_{mn}^2 - \omega^2)\alpha_m \alpha_n} \times (\cos \alpha_m x_0 - \cos \alpha_m x_a)(\cos \alpha_n y_0 - \cos \alpha_n y_b). \quad (33)$$

Eqs. (31) and (33) actually give solutions for forced vibration of the thin plate driven by dual piezoelectric actuator via lines and via areas, respectively.

In the following, we deal with the continuity conditions between the actuators and the plates, so that the equivalent electric networks for the piezoelectric actuators and the thin plate will be accomplished. At first, we assume two approximate hypotheses as follows:

Hypothesis 1. At the interfacial surfaces between the thin plate and the piezoelectric actuators shown in Fig. 4, the actual distributed activations are approximately equivalent to the activation given by Eq. (14) or (19) as shown in Fig. 3a or 3b. In other words, the representations of average bending moments per unit length or per unit area have a good simulation of actual distributed bending activations given by Eq. (13). It will be found in the numerical examples of Section 4 that this hypothesis leads to quiet accurate results and is more convenient to analysis.

Hypothesis 2. The displacement continuity conditions are approximately satisfied at the interface between thin plates and piezoelectric actuators, which can be analyzed according to the following procedures. At first, according to the theory of thin plates [22], the relationships between the in-plane displacements and the deflection of the plate are

$$u_s = -z\frac{\partial w_s}{\partial x}, \quad v_s = -z\frac{\partial w_s}{\partial y}. \quad (34)$$

It is recognized that Eq. (34) are fulfilled everywhere inside the thin plate, i.e., $-t_s/2 \leqslant z \leqslant t_s/2$. But we approximately expand Eq. (34) into the region of $-(t_s + t_p)/2 \leqslant z \leqslant (t_s + t_p)/2$. Therefore, the displacements of the actuators can be related with the deflection of the thin plate, i.e.,

$$u_p = -\frac{t_s + t_p}{2}\frac{\partial w_s}{\partial x}, \quad v_p = -\frac{t_s + t_p}{2}\frac{\partial w_s}{\partial y}. \quad (35)$$

At last, the velocities at the four points on the interfacial lines between the plate and actuators can be defined as mechanical flows,

$$U_{s1} = -\frac{t_s + t_p}{2} \left.\frac{\partial^2 w_s}{\partial x \partial t}\right|_{x=x_0}^{y=y^*}, \quad U_{s2} = -\frac{t_s + t_p}{2} \left.\frac{\partial^2 w_s}{\partial x \partial t}\right|_{x=x_a}^{y=y^*},$$
$$U_{s3} = -\frac{t_s + t_p}{2} \left.\frac{\partial^2 w_s}{\partial y \partial t}\right|_{x=x^*}^{y=y_0}, \quad U_{s4} = -\frac{t_s + t_p}{2} \left.\frac{\partial^2 w_s}{\partial y \partial t}\right|_{x=x^*}^{y=y_b} \tag{36}$$

where $x^* = (x_0 + x_a)/2$ and $y^* = (y_0 + y_a)/2$ are the x- and y-axial coordinate of A, B, C and D points shown in Fig. 4. In short, this hypothesis says that the extension (or contraction) velocity of piezoelectric actuators equals to product of the rotating velocity of the thin plate and the distance between the mid-plane of the top or bottom actuator and the thin plate. A, B, C and D points shown in Fig. 4 are approximately representative of the displacements continuity conditions, so that the following relations of the displacements continuity conditions are implied, that is,

$$\mathbf{U}_s = \mathbf{U}_a, \tag{37}$$

where

$$\mathbf{U}_a = \{U_1, U_2, U_3, U_4\}^{\mathrm{T}},$$
$$\mathbf{U}_s = \{U_{s1}, U_{s2}, U_{s3}, U_{s4}\}^{\mathrm{T}}. \tag{38}$$

In the above equations, $U_i, (i = 1, 2, 3, 4)$ are defined by Eq. (4) for piezoelectric actuators while $U_{si}, (i = 1, 2, 3, 4)$ are defined as mechanical flows by Eq. (36) in terms of the deflection of the plate.

In the remains of this section, the system impedance of the thin plate containing the 2D piezoelectric actuators will be analyzed. At first, using Eqs. (31) and (36), a linear relationship between the mechanical efforts and the mechanical flows of the thin plate is obtained, in admittance form,

$$\mathbf{U}_s = \mathbf{Y}_B \mathbf{F}_{pb}, \tag{39}$$

where $\mathbf{Y}_B$ is a 4×4 admittance matrix; or in impedance form,

$$\mathbf{F}_{pb} = \mathbf{Z}_{SB} \mathbf{U}_s, \tag{40}$$

where $\mathbf{Z}_{SB}$ is a 4×4 impedance matrix. The equivalent electric circuit of the thin plate is a four-port network show in Fig. 5a.

Similarly, the impedance matrices of the thin plate activated by the area activation bending can be obtained by using Eqs. (33) and (36), that is a 2×4 primitives matrix,

$$\mathbf{U}_s = \mathbf{Y}_C \mathbf{F}_{pc}, \tag{41}$$

or a 2×4 impedance matrix,

$$\mathbf{F}_{pc} = \mathbf{Z}_{SC} \mathbf{U}_s. \tag{42}$$

Eq. (41) or (42) shows that the equivalent electric circuits of the thin plate is a four-port network with two short circuit as shown in Fig. 5b in this case. In the two equations of Eqs. (39) and (41), $\mathbf{Y}_B$ and $\mathbf{Y}_C$ can be conveniently calculated using Eqs. (31) and (33) with a certain number of m and n, respectively.

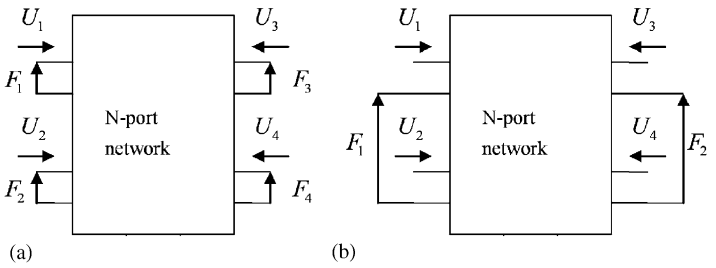

Fig. 5. Equivalent electric networks for the thin plate: (a) vibration driven by the piezoelectric actuators producing line bending moments; (b) vibration driven by the piezoelectric actuators producing area bending moments.

In order to obtain the system impedance, we will solve the combined equations of the impedance of piezoelectric actuators and thin plate in the following.

The impedance equation of dual line actuators shown in Eq. (16) can be rewritten in forms of block arrays,

$$\begin{Bmatrix} \mathbf{F}_{pb} \\ V \end{Bmatrix} = \begin{bmatrix} \mathbf{Z}_{Baa} & \mathbf{Z}_{Bab} \\ \mathbf{Z}_{Bba} & \mathbf{Z}_{Bbb} \end{bmatrix} \begin{Bmatrix} \mathbf{U}_a \\ I \end{Bmatrix}, \tag{43}$$

where $\mathbf{Z}_{Baa}$, $\mathbf{Z}_{Bab}$, $\mathbf{Z}_{Bba}$ and $\mathbf{Z}_{Bbb}$ are sub-blocks of $\mathbf{Z}_B$ and of 4×4, 4×1, 1×4 and 1×1 impedance matrices, respectively. Solving the equations of Eqs. (43) and (39) together with Eq. (37) yields

$$P^* = \mathbf{Z}_{Bba}\mathbf{Y}_B(\mathbf{I} - \mathbf{Z}_{Baa}\mathbf{Y}_B)^{-1}\mathbf{Z}_{Bab} + \mathbf{Z}_{Bbb}, \tag{44}$$

where $\mathbf{I}$ is a 4×4 unit array, and P^* denotes the system impedance, which is defined as

$$P^* = V/I. \tag{45}$$

Similarly, the impedance equation shown in Eq. (21) of dual 2D piezoelectric area actuators is rewritten in forms of block arrays,

$$\begin{Bmatrix} \mathbf{F}_{pc} \\ V \end{Bmatrix} = \begin{bmatrix} \mathbf{Z}_{Caa} & \mathbf{Z}_{Cab} \\ \mathbf{Z}_{Cba} & Z_{Cbb} \end{bmatrix} \begin{Bmatrix} \mathbf{U}_a \\ I \end{Bmatrix}, \tag{46}$$

where $\mathbf{Z}_{Caa}$, $\mathbf{Z}_{Cab}$, $\mathbf{Z}_{Cba}$ and $\mathbf{Z}_{Cbb}$ are sub-blocks of $\mathbf{Z}_C$ and of 2×4, 2×1, 1×4 and 1×1 impedance matrix. Solving the equations of Eqs. (46) and (41) with the consideration of Eq. (37) leads to

$$P^* = \mathbf{Z}_{Cba}\mathbf{Y}_C(\mathbf{I} - \mathbf{Z}_{Caa}\mathbf{Y}_C)^{-1}\mathbf{Z}_{Cab} + \mathbf{Z}_{Cbb}, \tag{47}$$

where $\mathbf{I}$ is a 2×2 unit array. In fact, Eqs. (44) and (47) give two equivalent electric circuit representations for thin plate with 2D piezoelectric actuators. Once the system impedance is obtained, all physical fields in the thin plate and the piezoelectric actuators can be calculated, using Eqs. (7) and (31) or Eq. (33), if necessary.

4. Numerical examples

Let us consider a rectangle thin steel plate; two pieces of piezoelectric actuators are adhered on the upper and the lower surface of the plate. The analysis will be focused on the dynamic behavior of the smart plate under the conditions, where the actuators will be placed on different positions of the plate. The geometric configurations of the thin plate actuated by dual 2D piezoelectric actuators are shown in Fig. 6, which were investigated by Dimitriadis, Rogers and their co-workers [8] before. The materials and geometry parameters concerned are listed in Table 1. The thin plate is simply supported along the four edges of the plate. The resonant frequencies of this steel plate are calculated using Eq. (28) and listed in Table 2.

Firstly, the dynamic behavior of the structure corresponding to configuration A, in which $x_0 = 0.32\,\mathrm{m}, x_a = 0.36\,\mathrm{m}, y_0 = 0.04\,\mathrm{m}, y_b = 0.26\,\mathrm{m}$ are calculated using Eqs. (44) and (47), respectively. The frequency response is drawn in Fig. 7 as the working frequency range from 100 to 2000 rad/s. It can be seen from Fig. 7 that the actuation will induce the resonant vibration near the frequency at 300, 940 and 1790 rad/s. Comparing with the frequencies listed in Table 2,

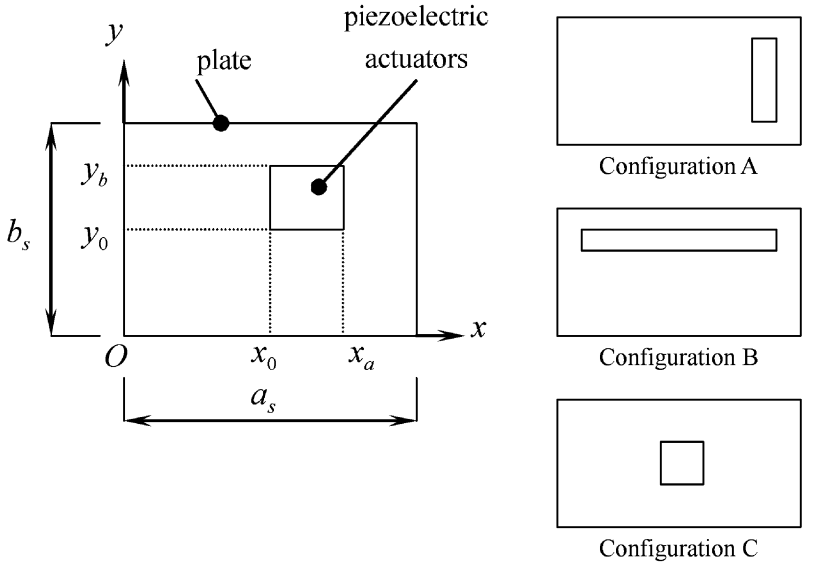

Fig. 6. The configurations of the numerical examples.

Table 1
The parameters of thin steel plate and piezoelectric polymer

	Density (kg/m^3)	Young's modules (GPa)	Poisson's ratio	Length (m)	Width (m)	Thickness (mm)
Plate	7870	207	0.292	0.38	0.30	1.5876
PVDF	2700	2.0	0.25			0.05
$d_{31} = d_{32} = 151 \times 10^{-7}$ V/m $\mu_{33} = 0.1062 \times 10^{-9}$ F/m						

Table 2
The resonant frequenies of simply supported plate ω_{mn}(rad/s)

n	(m)				
	1	2	3	4	5
1	437.5	1246.0	2592.5	4480.0	6905.5
2	941.4	1749.9	3097.4	4982.9	7409.4
3	1781.2	2589.7	3937.2	5822.7	8249.2
4	2957.0	3765.5	5112.0	6999.5	9425.0
5	4468.8	5277.3	6624.8	8511.3	10936.7

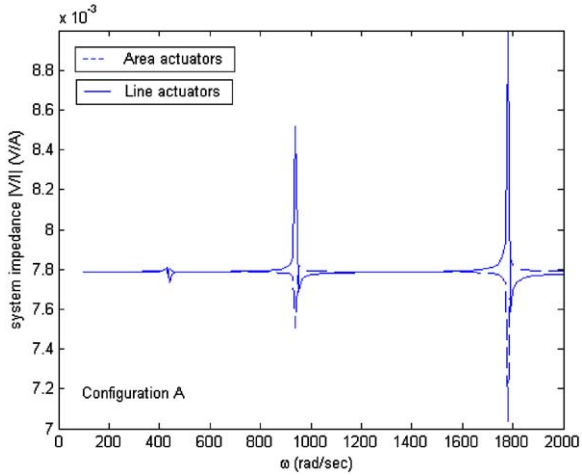

Fig. 7. The system impedance of the thin plate with a pair of PVDF actuators (Configuration A).

the corresponding resonant vibration modes should be $(m, n) = (1, 1)$, (2,1) and (3,1). These results are completely in agreement with the results shown by Figs. 4 and 7 in Ref. [8]. It is said that the vibration along y-axis direction will remain a peak during working frequency that varied from 100 to 2000 rad/s while the vibration along x-axis direction will change from one peak to three peaks at the same time.

Secondly, the dynamic characteristic of this plate in Configuration B is investigated. The piezoelectric actuators in Configuration B are rotated 90° in clockwise direction from Configuration A, that is in the position: $x_0 = 0.04\,\text{m}, x_a = 0.34\,\text{m}, y_0 = 0.23\,\text{m}, y_b = 0.27\,\text{m}$. Following the same solving procedure, the system impedance is obtained in Fig. 8 using line-bending actuator formulation Eq. (44) and area-bending actuator formulation Eq. (47), respectively. In the frequency under investigation, the two piezoelectric actuators in Configuration B only produce two resonant frequencies near 430 and 1240 rad/s. Thus, there will be two types of resonant vibrations. By examining Table 2, these two x–y

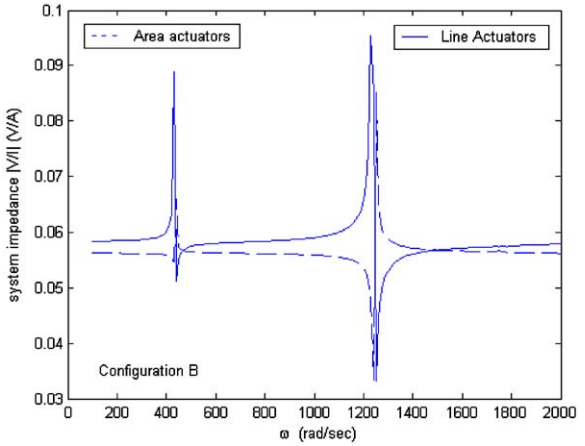

Fig. 8. The system impedance of the thin plate with a pair of PVDF actuators (Configuration B).

resonant modes should be (1,1) and (1,2), respectively, this conclusion was also shown in Fig. 8 of Ref. [8]. It can be found that the vibration along x-axis direction keeps one peak during the working frequency at 930 rad/s. In the other words, although the resonant frequency of the plate 941 rad/s corresponding to (2,1) is lower than the frequency 1246 rad/s corresponding to (1,2) in Table 2, the actuators in Configuration B cannot produce the thin plate vibration at the $(m = 2, n = 1)$ mode.

The third example is that two small piezoelectric actuators are centered in the thin plate shown in Configuration C of Fig. 6. The position and the size of the actuators are defined as $x_0 = 0.16\,\text{m}, x_a = 0.22\,\text{m}, y_0 = 0.13\,\text{m}, y_b = 0.17\,\text{m}$. The dynamic response curve is drawn in Fig. 9 of this paper. It is seen from the figure that these actuators actuate the thin plate an intensive resonant at the $(m = 1, n = 1)$ mode. Another resonant frequency is near 1780 rad/s. It has been found that the vibration along x direction has already shown two peaks while $\omega = 600\,\text{rad/s}$, i.e. $m = 2$. Examining Table 2, the resonant modes in this case should be (1,1) and (2,2) modes, respectively. But, as far as the vibration mode of $(m = 2, n = 1)$ is concerned, the position of the actuators are center located and are across the line of vibration mode (2,1). Therefore, most of the response is still accumulated on the vibration mode (1,1) although the working frequency approaches the resonant frequency for mode (2,1). The results shows that the actuators located in Configuration C cannot produce resonant vibration for mode (2,1) or (1,2). As the working frequency jumps to a frequency higher than 600 rad/s, the centered located actuators will actuate the symmetry vibration modes such as $(m = 1, 3, 5 \ldots n = 1, 3, 5 \ldots)$ which will almost produce no contribution to the vibration at the anti-symmetry vibration modes such as $(m = 2, 4, 6 \ldots n = 2, 4, 6 \ldots)$.

At last, the vibration of a simply supported thin plate driven by a pair of PZT-5A actuators are restudied here, which has been theoretically and experimental studied by Zhou, Rogers and their co-workers [9]. The thin plate is made of aluminum, whose size is 305 mm × 203 mm × 1.53 mm; and the two PZT patches are of 51 mm × 51 mm × 0.19 mm in size, which is located in the position: $x_0 = 0.025\,\text{m}$, $x_a = 0.067$, $y_0 = 0.051\,\text{m}$, $y_b = 0.102\,\text{m}$. More information about the

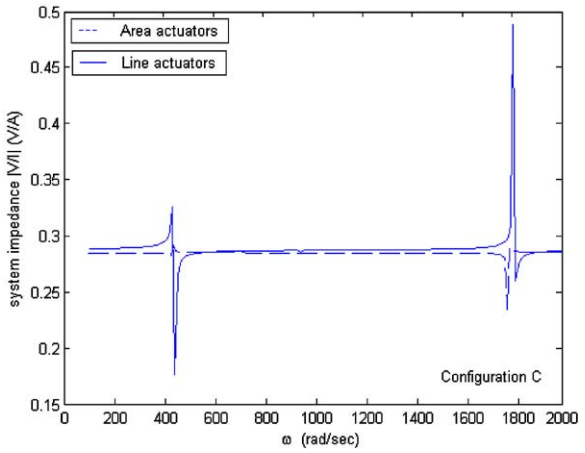

Fig. 9. The system impedance of the thin plate with a pair of PVDF actuators (Configuration C).

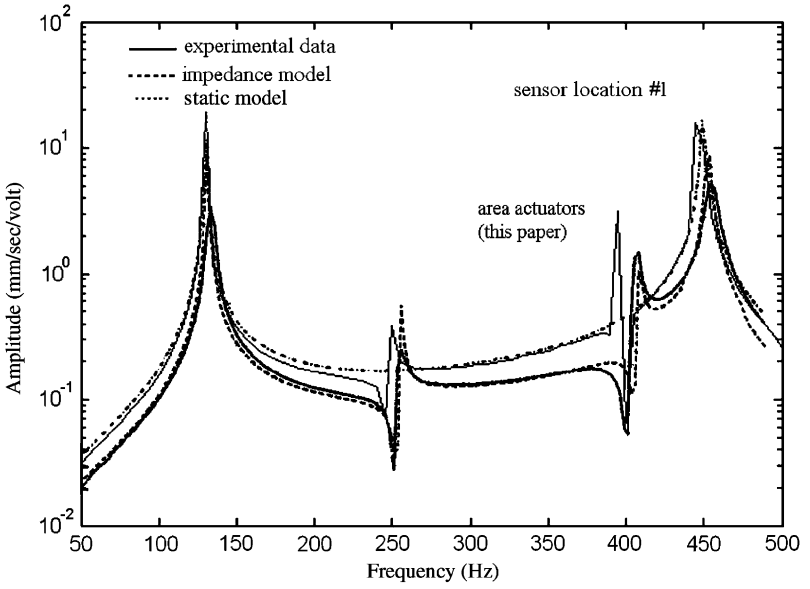

Fig. 10. The velocity response of a PZT actuator-driven plate at sensor location ♯1.

material properties and the experimental setup of this example can be found in Ref. [9]. During their vibration test, they measured the dynamic response using non-contact laser sensor at two different locations, that is, location ♯1: $x = 152\,\text{mm}$, $y = 102\,\text{mm}$, and location ♯2: $x = 229\,\text{mm}$, $y = 102\,\text{mm}$. We picked up the data from Ref. [9] in the coordinate system shown in Fig. 4 and then calculated the velocity response at sensor location ♯1 and sensor location ♯2 using Eqs. (47) and (33). The results obtained are plotted in Figs. 10 and 11, for vibration

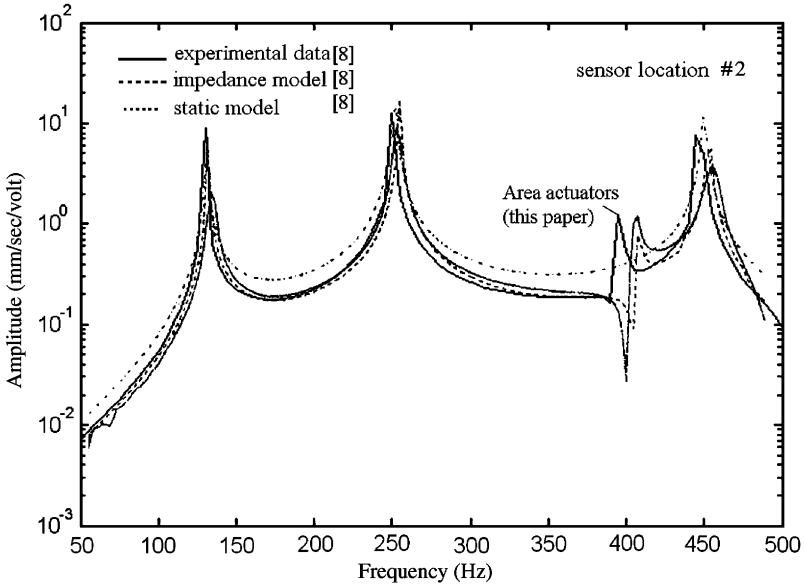

Fig. 11. The velocity response of a PZT actuator-driven plate at sensor location #2.

amplitude at sensor location #1 and sensor location #2, respectively. It can be seen from these figures that the models and computational methods proposed in this paper are quiet reliable and accurate.

5. Conclusions and discussions

Electric equivalent circuits for a thin plate with two-dimensional piezoelectric actuators are presented in this paper. The dynamical characteristics of 2D actuators producing forces actuation can be represented by a five-port electric network, and characteristics of a pair of 2D actuators producing pure bending actuation should be electrically equivalent to a five-port electric circuit with or without short close circuits. Under two approximate hypotheses, the actual activations and the displacement continuity on the contact surfaces between thin plate and 2D actuators are simply modeled. The results of numerical examples reveal that the two hypotheses we proposed in this paper are reasonable and practicable. The equivalent electric circuits for a thin plate with 2D piezoelectric actuators are finally obtained. The results of numerical examples show that the frequency characteristics of the considered problems coincide with the results reported earlier by other researchers. These facts demonstrate that it is capable of simulating complex electromechanical systems such as plates and shells with 2D piezoelectric actuators using equivalent electric circuits.

Although the concise formulations presented in this paper is only for the simply supported thin plates with 2D piezoelectric actuator, the method proposed here is capable of analyzing thin plates

with various kinds of boundary conditions. For the plates with clamped or free boundary conditions, some numerical methods such as FEM may be used to calculate the impedance matrix of the plate shown in Eqs. (40) and (42), and the framework of the equivalent electric network model we presented is applicable as well.

Further study on the equivalent electric network models for smart structures with piezoelectric elements will be needed to improve its accuracy and completeness. For examples, the two explicit hypotheses proposed here are the key to establish the equivalent electric networks, and the study on experimental verification of displacement continuous conditions shown in Eq. (34) should be a good job in the future. However, the advantage of the equivalent electric network models for smart structures are obvious. Since the analogy relationships between the real system and the virtual equivalent system are explicitly defined in the models, it is potential to develop equivalent electric simulation experiments for the smart structures mentioned above. Lastly, it will be more convenient to analyze and control the equivalent electric system using modern control theories including cybernetics than to do it directly on real smart structures.

Acknowledgements

This research was supported by the National Natural Science Foundation of China (No. 10172036). The authors wish to thank Prof. Yu-Ying Huang and Shu-Ping Liang for their valuable suggestion and Mr. Peng Hu and Dr. Ding-Gen Li for their help in analyzing electric networks in numerical examples.

Appendix A

The relation between electric current and the mechanical flows is

$$I = \mathrm{j}\omega C_p V + N_1(U_2 - U_1) + N_2(U_4 - U_3), \tag{A.1}$$

where

$$C_p = \frac{a_p b_p}{t_p}\left[\mu_{33} - \frac{Y_p^E}{1-v_p^2}(d_{31} - v_p d_{32})d_{31} - \frac{Y_p^E}{1-v_p^2}(d_{32} - v_p d_{31})d_{32}\right], \tag{A.2}$$

with

$$N_1 = \frac{Y_p^E b_p}{1-v_p^2}(d_{31} - v_p d_{32}),$$
$$N_2 = \frac{Y_p^E a_p}{1-v_p^2}(d_{32} - v_p d_{31}). \tag{A.3}$$

The elements of the impedance matrix $\mathbf{Z}_A$ are:

$$
\begin{aligned}
&Z_{A11} = (t_p k_p c_1 C_p/s_1 + N_1 d_a) C_0 Y_0,\\
&Z_{A12} = (-t_p k_p C_p/s_1 + N_1 d_a) C_0 Y_0,\\
&Z_{A13} = (t_p v_p C_p/b_p + N_2 d_a) C_0 Y_0,\\
&Z_{A14} = (-t_p v_p C_p/b_p + N_2 d_a) C_0 Y_0,\\
&Z_{A21} = (-2t_p k_p c_1^2 C_p/s_1 + t_p k_p C_p/s_1 + N_1 d_a) C_0 Y_0,\\
&Z_{A22} = (t_p k_p c_1 C_p/s_1 + N_1 d_a) C_0 Y_0,\\
&Z_{A23} = (-2t_p v_p c_2 C_p/b_p + t_p v_p C_p/b_p + N_2 d_a) C_0 Y_0,\\
&Z_{A24} = (t_p v_p C_p/b_p + N_2 d_a) C_0 Y_0,\\
&Z_{A31} = (t_p v_p C_p/a_p + N_1 d_b) C_0 Y_0,\\
\text{area}\quad &Z_{A32} = (-t_p v_p C_p/a_p + N_1 d_b) C_0 Y_0,\\
&Z_{A33} = (t_p k_p c_2 C_p/s_2 + N_2 d_b) C_0 Y_0,\\
&Z_{A34} = (-t_p k_p C_p/s_2 + N_2 d_b) C_0 Y_0,\\
&Z_{A41} = (-2t_p v_p c_1 C_p/a_p + t_p v_p C_p/a_p + N_1 d_b) C_0 Y_0,\\
&Z_{A42} = (t_p v_p C_p/a_p + N_1 d_b) C_0 Y_0,\\
&Z_{A43} = (-2t_p k_p c_2^2 C_p/s_2 + t_p k_p C_p/s_2 + N_2 d_b) C_0 Y_0,\\
&Z_{A44} = (t_p k_p c_2 C_p/s_2 + N_2 d_b) C_0 Y_0,\\
&Z_{A15} = Z_{A25} = d_a C_0 Y_0, \quad Z_{A35} = Z_{A45} = -d_b C_0 Y_0,\\
&Z_{A51} = -Z_{A52} = N_1 C_0, \quad Z_{A53} = -Z_{A54} = N_2 C_0,\\
&Z_{A55} = C_0,
\end{aligned}
\tag{A.4}
$$

where

$$
\begin{aligned}
&Y_0 = \frac{Y_p}{1 - v_p^2}, \quad C_0 = -\frac{\mathrm{i}}{\omega C_p},\\
&d_a = d_{31} + v_p d_{32}, \quad d_b = v_p d_{31} + d_{32},\\
&s_1 = \sin(a_p k_p), \quad s_2 = \sin(b_p k_p),\\
&c_1 = \cos(a_p k_p), \quad c_2 = \cos(b_p k_p).
\end{aligned}
\tag{A.5}
$$

The elements of the impedance matrix $\mathbf{Z}_C$ are:

$$
\begin{aligned}
&Z_{C11} = -(2t_p c_1 C_p/a_p - t_p C_p/a_p - N_1 d_a) C_0 Y_0,\\
&Z_{C12} = (t_p C_p/a_p + N_1 d_a) C_0 Y_0,\\
&Z_{C13} = -(2t_p v_p c_2 C_p/b_p - t_p v_p C_p/b_p - N_2 d_a) C_0 Y_0,\\
&Z_{C14} = (t_p v_p C_p/b_p + N_2 d_a) C_0 Y_0,\\
&Z_{C21} = -(2t_p v_p c_1 C_p/a_p - t_p v_p C_p/a_p - N_1 d_b) C_0 Y_0,
\end{aligned}
$$

$$
\begin{aligned}
&Z_{C22} = (t_p v_p C_p/a_p + N_1 d_b) C_0 Y_0,\\
&Z_{C23} = -(2t_p c_2 C_p/b_p - t_p C_p/b_p - N_2 d_b) C_0 Y_0,\\
&Z_{C24} = (t_p C_p/b_p + N_2 d_b) C_0 Y_0,\\
&Z_{C15} = -d_a C_0 Y_0, \quad Z_{C25} = -d_b C_0 Y_0,\\
&Z_{C31} = -Z_{C32} = N_1 C_0, \quad Z_{C33} = -Z_{C34} = N_2 C_0,\\
&Z_{C35} = C_0.
\end{aligned} \tag{A.6}
$$

References

[1] E.F. Crawley, J. Luis, Use of piezoelectric actuators as elements of intelligent structures, *AIAA Journal* 25 (10) (1987) 1373–1385.

[2] C. Park, C. Walz, I. Chopra, Bending and torsion models of beams with induced-strain actuators, *Smart Material Structure* 5 (1996) 98–113.

[3] C.W. Lim, L.H. He, Exact solution of a compositionally graded piezoelectric layer under uniform stretch, bending and twisting, *International Journal of Mechanical Engineering* 43 (2001) 2279–2292.

[4] C. Liang, F.P. Sun, C.A. Rogers, An impedance method for dynamic analysis of active materials systems, *Journal of Intelligent Material Systems and Structures* 8 (1997) 718–732.

[5] S. Zhou, C. Liang, C.A. Rogers, Integration and design of piezoelectric elements in intelligent structures, *Journal of Intelligent Material Systems and Structures* 6 (1995) 733–743.

[6] S. Zhou, C.A. Rogers, Power flow and consumption in piezoelectrically actuated structures, *AIAA Journal* 33 (7) (1995) 1305–1311.

[7] C. Liang, F.P. Sun, C.A. Rogers, Determination of design of optimal actuator location and configuration based on actuator power factor, *Journal of Intelligent Material Systems and Structures* 6 (1995) 456–464.

[8] E.K. Dimitriadis, C.R. Fuller, C.A. Rogers, Piezoelectric actuators for distributed vibration excitation of thin plates, *Journal of Vibration and Acoustics* 113 (1991) 100–107.

[9] Su-Wei Zhou, Chen Liang, C.A. Rogers, Impedance-based system modeling approach for induced strain actuator-driven structures, *Journal of Vibration and Acoustics* 118 (1996) 323–331.

[10] D.K. Cheng, *Analysis of Linear Systems*, Addison-Wesley, USA, 1959.

[11] C. Green, *Vibrations Manual*, Springfield NTIS, USA, 1971.

[12] R. Aoyagi, H. Tanaka, Equivalent circle analysis of piezoelectric bending vibrators, *Japanese Journal of Applied Physics* 33 (Part 1, 5B) (1994) 3010–3014.

[13] H. Tanaka, R. Aoyagi, Analysis of piezoelectric bending accelerometer using the equivalent circuit, *Japanese Journal of Applied Physics* 35 (Part 1, 5B) (1996) 3035–3037.

[14] Li Guo-Qing, Chen Chuan-Yao, et al. An equivalent circuit model for intelligent structures and its application to a smart beam with PZT actuator, *Acta Mechanica Solida Sinica* (1999) 343–348 (in Chinese).

[15] Li Guo-Qing, Study on Electromechanical Coupling Models and the Relevant Computation Methods for Smart Structures containing Piezoelectric Materials, *Ph.D. Dissertation*, Huazhong University of Science and Technology, Wuhan, China, May 2003 (in Chinese).

[16] Young S. Cho, Y. Eugene Pak, Chang S. Han, Sung K. Ha, Five-port equivalent electric circuit of piezoelectric bimorph beam, *Sensors and Actuators* 84 (2000) 140–148.

[17] C.W. Lim, L.H. He, Three dimensional electromechanical response of a parallel piezoelectric bimorph, *International Journal of Solids and Structures* 38 (2001) 2833–2849.

[18] H.S. Tzou, C.I. Tseng, Distributed piezoelectric sensor/actuator design for dynamic measurement/control of distributed parameter systems. A piezoelectric finite element approach, *Journal of Sound and Vibration* 138 (1) (1990) 17–34.

[19] Sung Kyu Ha, et al., Finite element analysis of composite structures containing distributed piezoceramics sensors and actuators, *AIAA Journal* 30 (3) (1992) 772–782.

[20] M. Brissaud, Rectangle piezoelectric plate loaded on each face: a three-dimensional approach, *Ultrasonics* 34 (1996) 87–90.
[21] E.F. Crawley, K.B. Lazarus, Induced strain actuation of isotropic and anisotropic plates, *AIAA Journal* 29 (6) (1997) 944–950.
[22] S. Timoshenko, S. Woinowsky-Krieger, *Theory of Plates and Shells*, McGraw-Hill Book Company Inc., New York, 1959, pp. 180–229.